A EUROPEAN JOURNAL OF CHEMICAL BIOLOGY

CHEMBIOCHEM

SYNTHETIC BIOLOGY & BIO-NANOTECHNOLOGY

# Accepted Article

**Title:** Mammalian Cell-driven Polymerisation of Pyrrole

**Authors:** Harry G Sherman, Akhil Jain, Jacqeuline Hicks, Snow Stolnik, Cameron Alexander, and Frankie James Rawson



**To be cited as:** *ChemBioChem* 10.1002/cbic.201800630

**Link to VoR:** http://dx.doi.org/10.1002/cbic.201800630

A Journal of

ChemPubSoc Europe

WILEY-VCH

www.chembiochem.org

10.1002/cbic.201800630

WILEY-VCH

COMMUNICATION

# Mammalian Cell-driven Polymerisation of Pyrrole

Harry G. Sherman [a], Jacqueline M. Hicks [a], Akhil Jain [a], Jeremy J. Titman [b], Cameron Alexander, Snow Stolnik [a], and Frankie J. Rawson* [a]

Dedication ((optional))

**Abstract:** A model cancer cell line was used to initiate polymerisation of pyrrole to form the conducting material polypyrrole. The polymerisation was shown to occur via cytosolic exudates rather than via membrane redox sites which normally control the oxidation state of iron as ferricyanide or ferrocyanide.. The data demonstrate for the first time that mammalian cells can be used to initiate synthesis of conducting polymers, and suggest a possible route to detection of cell damage and/or transcellular processes via an in-situ and amplifiable signal generation.

Conducting polymers, such as polypyrrole, have numerous applications ranging from bio/sensing[1],[2] and activation of drug delivery[3], to 'smart' textiles[4], components in fuel cells[5], and in the bioelectronics field which constitutes the merging of biology with electronics. Conventional synthesis of polypyrrole can be performed using a metal catalyst such as ferricyanide (FIC)[6] (Figure 1a). However, it would be of interest for a number of bio-sensing and/or bioelectronic applications to carry out the synthesis of conducting polymers in the presence of cells, as a means to ensure the closest proximity of biological functionality and electrical conductance regions. The *in-situ* formation of synthetic polymers catalysed by live cellular activity has been demonstrated for the self-labelling of bacteria[7] and enhanced functional and chemical properties in yeast and bacteria [1],[8,9] In addition, *Saccharomyces cerevisiae*[10,11] has been reported to be able to mediate polymerisation of pyrrole. The analogous mammalian cell-instructed synthesis could have potential applications ranging from enhanced early stage cancer cell detection, in targeting of abnormal cells by in-situ cytotoxic polymer production, or polymer 'cell-painting' in order to induce immune system attack. However, to date, there have been no reports of mammalian cell initiated polymerisations. This is perhaps surprising, as for yeast-induced polymerisation it has been suggested that a cell trans plasma membrane transport system (tPMETS), such as an oxido-reductase, generates the active form of the catalyst ferrocyanide (FOC), and it is also known that cancer cells exhibit increased levels of tPMET to facilitate non-oxidative metabolism[12]. Accordingly, a focus for this work was the exploitation of redox processes in cancer cells to induce polymer synthesis in close proximity to the cell surface, as a first step to interfacing tumorigenic processes with an in-situ conduction/materials detection system.

Nevertheless, it should be noted that there are significant challenges for carrying out polymer synthesis in the vicinity of mammalian cells. This is because eukaryotic cells lack the protective cell wall that yeasts and bacteria have, and are unable to adapt to harsh environments in the way that bacteria can. Additionally, there is still a lack of evidence regarding the mechanism by which pyrrole is polymerised in the presence of yeast, with the suggestion that this occurs by tPMETS being incompletely tested. We therefore set out to test the hypothesis that polymerisation of pyrrole could be achieved with malignant mammalian cells, with a view to establishing a clearer mechanism by which this might occur in a range of cell types expressing tPMETS.

We report here the successful polymerisation of pyrrole in the presence of cancer cell suspensions, and describe a protocol for reporting the details of in-situ polymerisation and potential catalysis via tPMET. We also highlight the characterisation of surface oxidative capacity as a pre-requisite to understanding whether synthesis is indeed cell-surface or live cell mediated.

We performed initial experiments with *Saccharomyces cerevisiae* to confirm the literature observation that a eukaryote could mediate the polymerisation of pyrrole[10]. This data is shown in Figure S1, and confirmed polymer synthesis by the formation of a black precipitate in the presence of *Saccharomyces cerevisiae* (Figure S1a). To determine if malignant mammalian cells could be used to drive conducting polymer synthesis in-situ, we used the suspension leukaemia cell line, K562 cells. We chose a malignant cell line beacuse cancer cells are proposed to have increased levels of tPMET to facilitate non-oxidative metabolism[12]. There may therefore be potential applications to target cancer cells through hijacking tPMET mechanisms, in this case for polymer synthesis. Polymerisations were prepared with combinations of solutions containing FIC or FOC, K562 cells or no cells, and pyrrole or no pyrrole. Analysis of solutions exposed to these conditions were performed qualitatively by visual inspection, and quantitatively using ImageJ. This was performed to confirm if the formation of polypyrrole could be mediated by mammalian cell biology. Figure 1b and c show differences in colour between the sample solutions. Sample 1, had a dark black pellet with yellow-green colouration of the media. This indicated that the sample contained the active catalyst FIC, which presents a yellow-green colour, and that black precipitated particles of polypyrrole were produced. Sample 2, which contained only FOC and pyrrole, did show evidence of some autopolymerisation.

[a] Harry G. Sherman, Dr Jacqueline M. Hicks, Dr Akhil Jain, Prof.. Cameron Alexander, Dr, Snow Stolnik, Dr. Frankie J. Rawson*
School of Pharmacy, University Park,
University of Nottingham
Nottingham, NG7 2RD
E-mail: frankie.rawson@nottingham.ac.uk
[b] Jeremy J. Titman
School of Chemistry, University Park,
University of Nottingham
Nottingham, NG7 2RD, UK

Supporting information for this article is given via a link at the end of the document.

There was a small amount of black precipitate within the base of the centrifuge tube and the colour of the solution was light brown. However, when comparing Samples 3 and 6 (which

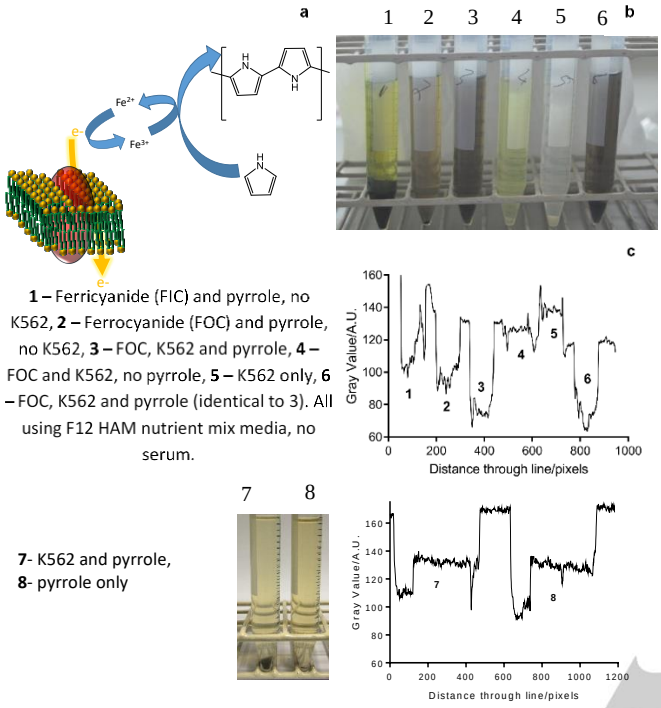


**Figure 1. Cell-mediated polymerisation of pyrrole by K562 cells** (a) Theoretical mechanism of polymerisation of pyrrole to polypyrrole. Trans plasma membrane oxidoreductases (tPMET) oxidoreductases at the plasma membrane oxidise potassium ferrocyanide (FOC) to potassium ferricyanide (FIC). FIC then accepts an electron from pyrrole, forming a radical and driving chemical synthesis of polypyrrole. The most accepted version for chemical synthesis is through the coupling and subsequent deprotonation of the pyrrole radical to form a bipyrrole. Re-oxidation, coupling, and deprotonation continue to form oligomers and finally PPy[13].(b) Polymerisation of pyrrole following 48 hour incubation at 37°C and 5% $CO_2$. Pelleted *via* centrifugation for 300g before imaging. (N = 3, n = 1) (c) ImageJ analysis of polymerisation vials within (b). (N = 3, n = 1).

contain inactive catalyst FOC, K562 cells and pyrrole) to the control Sample 2, it was clear that the cells induced formation of a precipitate. This was apparent firstly due to the black colouration of the pellets (**Figure 1b**), indicating polymer production. Furthermore, the pellets were of a greater size than those for the K562 cells-only control (Sample 5), indicating material had been produced. The gray value analysis (**Figure 1c**) also indicated that the suspensions of Sample 3 and 6 were ~20 A.U. darker compared to the control Sample 2, indicating polymerisation greater than the baseline autopolymerisation had occurred. The suspension was not darkened by the cells as the suspension had been centrifuged prior to images being taken. It is likely therefore that polypyrrole particles had been formed. Samples containing no pyrrole (Samples 4 and 5) showed no darkening of the media and a pale pellet indicative of cells only, indicating no polymer synthesis. This was corroborated in **Figure 1c**, which showed these samples had the lowest gray value. Of note was the yellow-green colour of Sample 4, which initially contained only FOC, which was clear or very pale yellow in colour. This is important as it demonstrated that oxidation of the clear FOC to yellow-green FIC was occurring. In order to assess the role of cells in driving the synthesis of polypyrrole in the absence of the iron catalyst, we also performed an additional control experiment where pyrrole was incubated with K562 cells and pyrrole (sample 7) or with pyrrole only (sample 8) (Figure 1c). Sample 7 yielded a grey pellet indicative that the cells could catalyse some level of pyrrole polymerisation in the absence of an iron catalyst. However, the pellet was much smaller and less dark than sample 1, indicating that less polypyrrole was being formed. No polypyrrole was observed in the supernatant of sample 7, and no difference in supernatant gray value was observed between samples 7 and 8 (Figure 1c). These data therefore suggested that the biologically instructed polymerisation without an iron catalyst (sample 7) occurred at slower rates than when the experiment was performed in the presence of the active iron catalyst (sample 1). To confirm the identity of the precipitate $^{13}$Carbon solid state nuclear magnetic resonance (NMR), scanning electron microscopy field emission gun (SEM-FEG) with energy-dispersive X-ray spectroscopy (EDX) analysis, and Fourier transform infrared spectroscopy (FTIR) assays were performed. The data from these experiments are shown in **Figure 2** and **Figure S2** (EDX). In **Figure 2a**, the solid state NMR spectra of both cell and non-cell mediated polypyrrole formation are shown. For each there was a distinctive peak at ~ 120 ppm. This is line with observations for $^{13}$C NMR spectra for polypyrrole by Forsyth et al[14]. This is consistent with a polypyrrole that is oxidised due to handling in air. The peak at ~20 ppm was undefined, and may suggest impurities in the polypyrrole produced. This peak was larger for the cell-incubated sample, which suggest the cell mediated polymerisation was less controlled. **Figure 2b and 2c** represent the FTIR spectra for non-cell mediated and cell mediated polymerisation, respectively. The data obtained were in line with recent structural characterisation of chemically synthesised polypyrrole using FTIR[15]. Detailed analysis of peak assignment can be found in the SI and Table SI1. There were evident differences between these FTIR spectra, which indicated changes in the vibrational characteristics of the produced polypyrrole for cellular-mediated polymerisation. SEM-FEG images were used to ensure that the polymerised structure was in line with the literature (**Figure 2d-g**). EDX analysis was also carried out to ensure a nitrogen signature for polypyrrole identification could be detected for structures identified as polypyrrole candidates (**Figure S2**). EDX data demonstrated nitrogen signatures in the polymerisation material visible in **Figure 2d-g**, but not in the background metal pin/material, providing further evidence the polymer is polypyrrole. Magnified (x95,000) SEM images showed the nanostructure of the polymer produced for non-cell mediated (**Figure 2d**) and cell mediated (**Figure 2e**) samples. The images obtained were similar to those observed previously[15–17]; a 5 kV operating voltage was used in line with two of these studies. The polypyrrole particles obtained were approximately 50–100 nm in diameter for both samples, and tended to aggregate into larger structures with irregular granular

10.1002/cbic.201800630




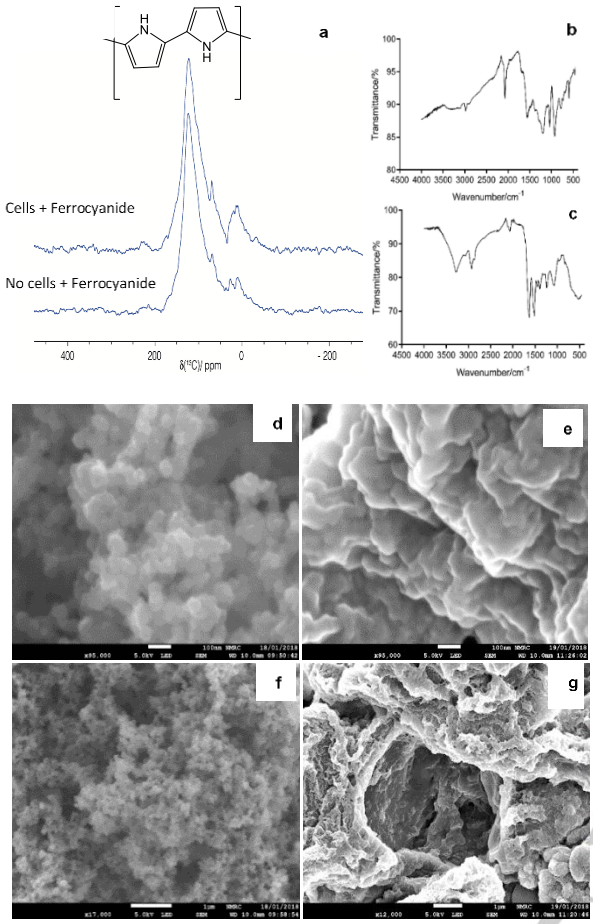


**Figure 2. Characterisation of non-cell (FIC) and cell (FOC and K562 cell) mediated polypyrrole.** (a) $^{13}C$ solid state nuclear magnetic resonance (NMR) spectrum for cell- and non-cell mediated polypyrrole. (b) Non-cell mediated Fourier transform infrared spectroscopy (FTIR) transmittance spectrum for polypyrrole. (c) Cell mediated FTIR transmittance spectrum for polypyrrole. (d) High magnification scanning electron microscopy (SEM) analysis, non-cell mediated. (e) High magnification SEM analysis, cell mediated. Coated with 10 nm iridium prior to imaging. (f) Lower magnification SEM analysis, non-cell mediated. Coated with 10 nm iridium prior to imaging. (g) Lower magnification SEM analysis, cell mediated. Coated with 10 nm iridium prior to imaging. (d-g) Imaged using 5.0 kV operating voltage.

morphology. These latter agglomerates were formed in both non-cell mediated (**Figure 2f**) and cell mediated (**Figure 2g**) experiments. Although the granular structure was still observable at high magnification for the cell mediated synthesis, the structures were smoothed (**Figure 2e**). This morphology was more apparent when observing the larger structure (**Figure 2g**) and comparing to non-cell mediated synthesis (**Figures 2d and f**). Others have noted this phenomenon[16] [18] and suggested this arises from redox changes in the polymer or due to doping. The slight shift to higher vibrational frequencies seen in the cell mediated polypyrrole FTIR also is in accord with similar observations by Geetha et al[18] comparing doped and undoped polypyrrole.

The confirmation that polypyrrole had been produced was the first indication that mammalian cells were capable of mediating the synthesis of a conductive polymer in-situ.

We were then interested in establishing mechanistic insights into the polymerisation. A series of assays were performed to determine if the polypyrrole produced was through tPMET. These data are shown in Figure 3. Figure 3a shows trypan blue analysis for the cells before and after 48 hours polymerisation. The viability and cell number at the start of the experiment were 94.5% and 1.0 x $10^8$ cells, respectively. Incubation with media only (K562 only sample) showed no change over the 48 hours, at 80% viability (Figure 2). The two polymerisation samples that included FOC, K562 cells and pyrrole showed a viability of 0%, and cell numbers of 6.3 and 6.5 x $10^8$ cells, respectively. The FOC and K562 incubated sample showed some reduction in both viability and cell number, at 41.5% and 3.4 x $10^8$ cells, respectively. These data indicated that the pyrrole and FOC were inducing some membrane damage to the cells. We decided to investigate how cell death was occurring, as in situ induced toxicity might be a further application of pyrrole electrochemistry in cancer cell biology[19]. To investigate whether the cell death was due to necrosis or from apoptosis, caspase 3/7 assays were performed on the samples after 48 hours of the polymerisation. The time point was selected to reflect the time frame of the polymerisation process. Cells were imaged immediately following polymerisation with a caspase assay kit. It was important to establish that the caspase assay reagent kit did not induce any significant cell death. This was ascertained by the lack of caspase activity observed in the cell only control (Figure 3 dii) when compared to cells exposed to pyrrole (Figure 3 b) where an increase in fluorescence is observed which is proportional to cell death which is induced the pyrrole . Therefore confirming the kit is biocompatible. Figures labelled (i) show the unstained control for background fluorescence, and (ii) indicates stained samples**. Figures 3b and e** show Samples 2 and 6 (the inactive catalyst (FOC)) incubated staining relative to their control. This meant that the reduction of viability to 0% that is observed for these samples is at least in part occurring by apoptosis. It also highlights variability during polymerisation. Stronger staining was observed in the FOC incubated sample, this may be due to the apoptotic process occurring closer to the time of imaging, as the viability for this sample was higher.

Minimal staining was observed for the K562 only sample (Sample 5) (**Figure 3d**), which is in line with the viability measurements. From these data we can infer that the polymerisation was not being mediated by redox control of FIC by a tPMET. This indicated that the polymerisation was mediated by intracellular components being effluxed and then engaging in electron transfer events with iron. It is also demonstrateds that cell death occured initially by apoptosis. To provide evidence if oxidative tPMET processes were occurring a previously characterised electrochemical assay[20] for studying cellular tPMET was used. K562 cells were incubated with either FIC or FOC. A significant upward shift in the linear sweep voltammogram was observed for 0.01 mM FIC incubation, indicating that the K562 cells were capable of reducing FIC (**Figure 3f**). K562 did not show any significant shift in cathodic current for 0.01 mM FOC incubation (Figure 3e).

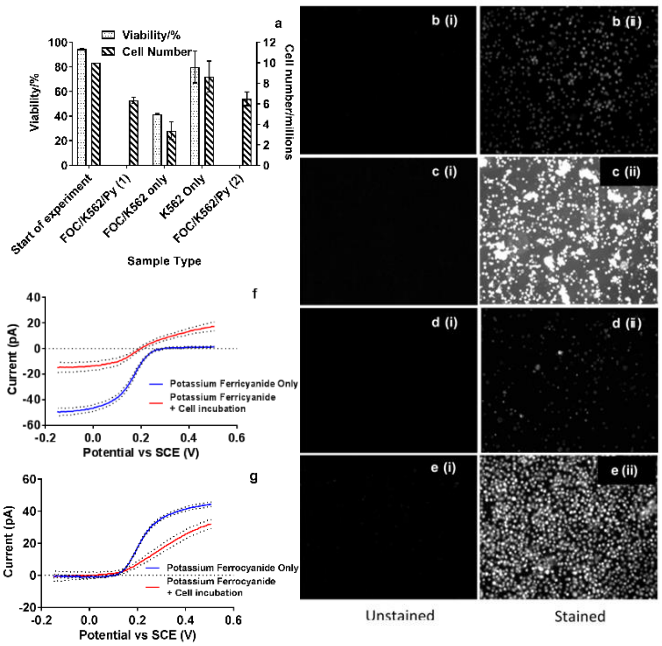


**Figure 3. Polypyrrole synthesis occurs via non-tPMET mediated electron transfer following partially apoptotic cell death**. (a) Trypan blue exclusion for cell viability and cell number following 48 hours polymerisation. (N = 2, n = 1) (b-e) Caspase 3/7 assay (CellEvent™ Caspase-3/7 Green Detection Reagent). (N = 2, n = 1) (b) Potassium ferrocyanide (FOC), pyrrole and K562 cells R1 (Sample 3). (c) FOC and K562 cells, no pyrrole (Sample 2). (d) K562 cells only (Sample 5). (e) FOC, pyrrole and K562 cells R2 (Sample 6) (f) Voltammogram for potassium ferricyanide (FIC) reduction by K562 cells. Dotted lines indicate error bars ± 1SEM. (N = 3, n = 2) (g) Voltammogram for FOC oxidation by K562 cells. Dotted lines indicate error bars ± 1SEM. (N = 3, n = 2) (h) FIC/FOC reduction/oxidation analysis. (N = 3, n = 2).

This shows that the K562 cells did not have oxidative functionality. The results obtained were surprising, as the data in clearly showed that FOC was being oxidised. In addition, Fenton reaction chemistry allows for hydrogen peroxide, which can be produced using tPMET enzymes, to interact with ferrous iron to produce ferric iron, although this can have toxic effects.

These data suggest that oxidation was not through tPMET, but through the action of cellular exudates. The implications of the data are that the use of mammalian cancer cells are suitable for driving polymerisation of pyrrole, but that this process occurs through cytosolic exudates catalysing the reaction. In the absence of iron, when cells were exposed to pyrrole only (Figure 1c), polymerisation was observed to occur but at low levels. Based on this, we can conclude that iron mediated synthesis of polypyrrole occurs because of redox interaction with the cell exudate molecule, and also in part due to direct polymerisation via a cell exudate. It is however important to note that this is definitive evidence polymerisation is via biological mediated control of the iron redox state.

The data highlight some unexpected mechanisms cellular polymerisation induced by eukaryotic and mammalian cells. We believe this work, to the best of our knowledge, is the first confirmation of the polymerisation of pyrrole using mammalian cells, albeit through mediation from intracellular components.

The indication that cell death was occurring initially via apoptosis suggests some directions for further research. Since pyrrole is toxic but polypyrrrole is cytocompatible, the detection of polypyrrole conductivity in the presence of cells might acts as a proxy indicator of metabolism or of cell death. Additionally the pyrrole/polypyrrole system might act as a 'reverse pro-drug', whereby through the killing of the cells and subsequent polymerisation, the toxic pyrrole is converted to a biocompatible polymer. Concentration profiles for FOC and pyrrole do suggest that viability is not always compromised specifically by pyrrole and FOC ((**Figure S3**), and so this may prove useful in the future as a means of killing cells in a specific locale while minimising surrounding cell toxicity. Additionally, polypyrrole formation and conductance might be a route to detection of cell damage and/or transcellular processes via an in-situ and amplifiable signal generation. Moreover, , the fact that the polymerisation occurs via biologically-mediated reactions, gives rise to an opportunity to interface in-situ grown conductive polymers with live cells similarly to that reported with non-conductive polymers [7], if an appropriate biocompatible monomer or concentration can be selected. +

To conclude, this study marks the first mammalian cell-driven polymerisation of polypyrrole.. This occurred through a process whereby membrane perturbation allowed cytosolic exudates to drive polymerisation by oxidising a metal catalyst. The research suggests a new paradigm for how conductive components may be interfaced with biology via a cell- instructed synthesis of conductive materials. This finding may be of particular importance for future applications in bioelectronics, as it enables a 'bottom up' approach to integrating the cellular components with conducting materials via generation of the electronic component in-situ

## Experimental Section

Detailed methods can be found in the supporting information

## Acknowledgements

This work was supported by the Engineering and Physical Research Council [grant numbers EP/L01646X, EP/R004072/1], The University of Nottingham CDT in Advanced Therapeutics and Nanomedicines, and Walgreens and Boots Alliance for financial support. The Nanoscale and Microscale Research Centre (nmRC) is thanked for access and technical support for SEM imaging.

**Keywords:** Mammalian • polypyrrole • keyword 3 • keyword 4 • keyword 5

[1] S. Radhakrishnan, S. Paul, *Sensors Actuators, B Chem.* **2007**, *125*, 60–65.
[2] A. Kausaite-Minkstimiene, V. Mazeiko, A. Ramanaviciene, A. Ramanavicius, *Sensors Actuators, B Chem.* **2011**, *158*, 278–285.
[3] S. Geetha, C. R. K. Rao, M. Vijayan, D. C. Trivedi, *Anal. Chim. Acta* **2006**, *568*, 119–125.
[4] E. Hakansson, A. Kaynak, T. Lin, S. Nahavandi, T. Jones, E. Hu, *Synth. Met.* **2004**, *144*, 21–28.
[5] C. Feng, L. Ma, F. Li, H. Mai, X. Lang, S. Fan, *Biosens. Bioelectron.* **2010**, *25*, 1516–1520.
[6] E. Andriukonis, A. Ramanaviciene, A. Ramanavicius, *Polymers (Basel).* **2018**, *10*, 749.
[7] E. P. Magennis, F. Fernandez-Trillo, C. Sui, S. G. Spain, D. J. Bradshaw, D. Churchley, G. Mantovani, K. Winzer, C. Alexander, *Nat. Mater.* **2014**, *13*, DOI 10.1038/nmat3949.
[8] R. Bin Song, Y. Wu, Z. Q. Lin, J. Xie, C. H. Tan, J. S. C. Loo, B. Cao, J. R. Zhang, J. J. Zhu, Q. Zhang, *Angew. Chemie - Int. Ed.* **2017**, *637551*, 10516–10520.
[9] J. Niu, D. J. Lunn, A. Pusuluri, J. I. Yoo, M. A. O'Malley, S. Mitragotri, H. T. Soh, C. J. Hawker, *Nat. Chem.* **2017**, *16*, 1–47.
[10] A. Ramanavicius, E. Andriukonis, A. Stirke, L. Mikoliunaite, Z. Balevicius, A. Ramanaviciene, *Enzyme Microb. Technol.* **2016**, *83*, 40–47.
[11] E. Andriukonis, A. Stirke, A. Garbaras, L. Mikoliunaite, A. Ramanaviciene, V. Remeikis, B. Thornton, A. Ramanavicius, *Colloids Surfaces B Biointerfaces* **2018**, *164*, 224–231.
[12] P. M. Herst, M. V. Berridge, *Biochim. Biophys. Acta - Bioenerg.* **2007**, *1767*, 170–177.
[13] Y. Tan, K. Ghandi, *Synth. Met.* **2013**, *175*, 183–191.
[14] M. Forsyth, V.-T. Truong, M. E. Smith, *Polymer (Guildf).* **1994**, *35*, 1593–1601.
[15] A. Kausaite-Minkstimiene, V. Mazeiko, A. Ramanaviciene, A. Ramanavicius, *Colloids Surfaces A Physicochem. Eng. Asp.* **2015**, *483*, 224–231.
[16] J. Rao, K. Geckeler, *Prog. Polym. Sci.* **2011**, *36*, 887–913.
[17] R. Cruz-Silva, E. Amaro, A. Escamilla, M. E. Nicho, S. Sepulveda-Guzman, L. Arizmendi, J. Romero-Garcia, F. F. Castillon-Barraza, M. H. Farias, *J. Colloid Interface Sci.* **2008**, *328*, 263–269.
[18] S. Geetha, D. C. Trivedi, *Mater. Chem. Phys.* **2004**, *88*, 388–397.
[19] S. Kasibhatla, B. Tseng, *Mol. Cancer Ther.* **2003**, *2*, 573–580.
[20] H. G. Sherman, C. Jovanovic, S. Stolnik, F. J. Rawson, *Anal. Chem.* **2018**, *90*, 2780–2786.

10.1002/cbic.201800630

WILEY-VCH



**Entry for the Table of Contents** (Please choose one layout)

Layout 1:

## COMMUNICATION

Mammalian cell-driven synthesis of conductive polypyrrole is performed with a model cancer cell line. This was achieved in-situ which could represent a new method of forming bioelectronic systems from a bottom up approach. We also present a new electrochemical method that sheds light on the mechanism of how cells instruct such polymerisation events.

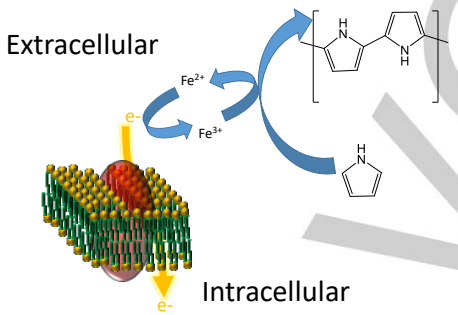


*Harry G. Sherman a, Jeremy J. Titman , Snow Stolnik , and Frankie J. Rawson* , Corresponding Author(s)**

**Mammalian Cell-driven Polymerisation of Pyrrole**

Layout 2:

## COMMUNICATION

((Insert TOC Graphic here))

*Author(s), Corresponding Author(s)**

***Page No. – Page No.***

**Title**

Text for Table of Contents